

Diffusion-weighted imaging (DWI) in musculoskeletal MRI: a critical review

Michael M. Y. Khoo · Philippa A. Tyler ·
Asif Saifuddin · Anwar R. Padhani

Received: 15 July 2010 / Revised: 11 November 2010 / Accepted: 13 January 2011 / Published online: 12 February 2011
© ISS 2011

Abstract Magnetic resonance imaging (MRI) is the mainstay of diagnosis, staging and follow-up of much musculoskeletal pathology. Diffusion-weighted magnetic resonance imaging (DWI) is a recent addition to the MR sequences conventionally employed. DWI provides qualitative and quantitative functional information concerning the microscopic movements of water at the cellular level. A number of musculoskeletal disorders have been evaluated by DWI, including vertebral fractures, bone marrow infection, bone marrow malignancy, primary bone and soft tissue tumours; post-treatment follow-up has also been assessed. Differentiation between benign and malignant vertebral fractures by DWI and monitoring of therapy response have shown excellent results. However, in other pathologies, such as primary soft tissue tumours, DWI data have been inconclusive in some cases, contributing little additional information beyond that gained from conventional MR sequences. The aim of this article is to critically review the current literature on the contribution of DWI to musculoskeletal MRI.

Keywords MRI · Diffusion MRI · Musculoskeletal diseases · Therapy response · Cancer

Introduction

Magnetic resonance imaging (MRI) is the mainstay of diagnosis, staging and follow-up of many musculoskeletal disorders. Conventional spin-echo, proton density and short tau inversion recovery (STIR) MRI sequences rely on the differing T1 and T2 relaxation characteristics of various pathological processes. Interpretations of the images are done qualitatively with analyses of signal intensity and morphology of anatomical structures on each of these sequences. However, some musculoskeletal diseases may have similar imaging characteristics, limiting the specificity of analyses, which can reduce diagnostic confidence.

Diffusion-weighted magnetic resonance imaging (DWI) is a recent addition to the musculoskeletal MR sequences being employed at many institutions. The signal intensity of DWI relies on the stochastic Brownian motion, or self-diffusion, of water molecules at a microscopic level within tissues. Extracellular water has more freedom, or is less impeded in its motion, in comparison to intracellular water molecules, which are limited in their motion by intracellular organelles, macromolecules and cell membranes. Water molecular diffusion on clinically acquired DWI sequences is therefore reflective of tissue organisational features, principally cellularity (number of cells per high power field). Areas with higher cellularity (and therefore more intracellular components and cell membranes) will demonstrate impeded molecular water mobility to a greater extent than areas where there has been loss of cellular integrity, such as areas of necrosis. DWI can therefore add functional information obtained at the cellular level to aid in the differentiation of normal and pathological tissues.

DWI as well as its variant diffusion tractography has established roles in neuro-imaging, where it is utilised in the assessment and detection of early cerebral ischaemia [1]

M. M. Y. Khoo (✉) · P. A. Tyler · A. Saifuddin
Department of Radiology, Royal National Orthopaedic Hospital,
Brockley Hill,
Stanmore, Middlesex HA7 4LP, UK
e-mail: Michael@khoo.me.uk

A. R. Padhani
Paul Strickland Scanner Centre, Mount Vernon Cancer Centre,
Northwood, UK

and other neurological pathologies including infection, neoplasia and demyelinating diseases [2]. It is relatively recently that musculoskeletal disorders have been evaluated by DWI. Some pathologies, including the differentiation between benign and malignant vertebral fractures [3] and the post-chemotherapy follow-up of tumours [4], have shown promising results. However, DWI assessment of other conditions has been equivocal in terms of added value over conventional imaging sequences [5]. For these reasons, the clinical situations in which DWI may be considered essential in the assessment of the musculoskeletal system need clarification. The aim of this review is to appraise the current literature on DWI in the musculoskeletal system in order to make recommendations on those situations where it could be considered an essential add-on to conventional MRI.

Basic principles of diffusion-weighted imaging

At human body temperature, random water molecules migrate approximately 30 μm over 50 ms, but only if there are no barriers to their motion. Because most human cells are in the same order of magnitude and sub-cellular structures have even smaller dimensions, the likelihood that tissue water molecules will encounter cellular components is extremely high. In fact it is highly likely that water molecules will have many interactions over such a short measurement interval. As a result, water movement in tissues is neither entirely free nor random, being modified by interactions with hydrophobic lipid-containing cell membranes, intracellular organelles, macromolecules and by-flows within tubular channels such as blood vessels and ducts. Thus tissue water motion is related to its microscopic structure. The thermally driven motion of water is uniquely assessed by DWI.

MRI is able to measure the water diffusivity by the application of diffusion sensitising gradients (motion probing gradients) to T2-weighted spin-echo sequences usually with echoplanar readouts of the data. Signal losses on DWI are proportional to both the free motion of water molecules and the diffusion gradient strength used [6, 7].

The strength and duration of application of diffusion sensitising gradients is indicated by their “b-value”. Generally, a range of b-values (two or more) are used in a DW-MRI study to interrogate the water diffusion properties of tissues. In the absence of diffusion sensitising gradients (b-value=0 s/mm^2), free water appears bright because of intrinsic T2-weighting. In images acquired with low b-values (50–100 s/mm^2), vessels and cerebrospinal fluid show marked signal attenuation because water molecules will have moved over a relatively large distance during the time of application of the diffusion sensitising gradients. Because signal intensity from blood vessels is attenuated on

low b-value images, these images are often termed “black blood” images (Fig. 1).

With increasing b-values, signal intensity attenuates steadily in other tissues, initially disappearing in free water (e.g. urine in the bladder), then in glandular tissues (e.g. prostate, salivary glands and pancreas) and then in tissues showing highly organised cellular structure such as the liver. Because water movement is relatively impeded in highly packed tissues such as tumours, very cellular tissues appear persistently bright against a darkening background at high b-values of 500–1,000 s/mm^2 . For the same reasons, several normal but highly cellular tissues also appear bright on high b-value images, including the brain, spinal cord, spleen (variable) and normal lymphatic tissues (tonsils, adenoids, lymph nodes). Thus, it can be seen that the signal intensity decay observed in tissues with increasing b-value generally follows a bi-exponential behaviour: the initial exponential behaviour is due to signal losses caused by blood flow, and the second exponent is due to extra-vascular, extra-cellular water movements.

Since tissue water movements are not free but impeded, tissue diffusivity is often termed the apparent diffusion coefficient (ADC; units: $\mu\text{m}^2/\text{s}$ or $\times 10^{-3} \text{mm}^2/\text{s}$). There are a number of measures of water diffusivity that can be used as biomarkers of tissue properties. These include relative signal intensity at different b-values, water diffusivity (D), apparent diffusion coefficient ($\text{ADC}_{\text{total}}$) and fractionated ADC (ADC_{fast} and ADC_{slow}). ADC_{fast} is calculated using low b-values (0–100 s/mm^2); it is dominated by the perfusion component of the total tissue diffusivity. At higher b-values (>100 s/mm^2), the perfusion component is largely extinguished, so ADC_{slow} measurements are more heavily determined by water diffusion within the cellular matrix. In most clinical studies, only $\text{ADC}_{\text{total}}$ is reported (usually simply written as ADC) so it is not possible to distinguish between the perfusion and non-perfusion components based on the quoted diffusivity. This is an important point to remember when interpreting clinical data with regards to lesion characterisation and therapy effects on tissues.

Techniques for DWI

Diffusion gradients can be applied to many standard MRI sequences, but the images produced are prone to artefacts resulting from physiological motions and eddy currents. Spin echo DWI sequences yield high signal-to-noise ratio (SNR) images and are more resistant to field inhomogeneity created by the application of diffusion gradients, but long acquisition times of several minutes limit their clinical use due to the increased likelihood of encountering motion-related artefacts.

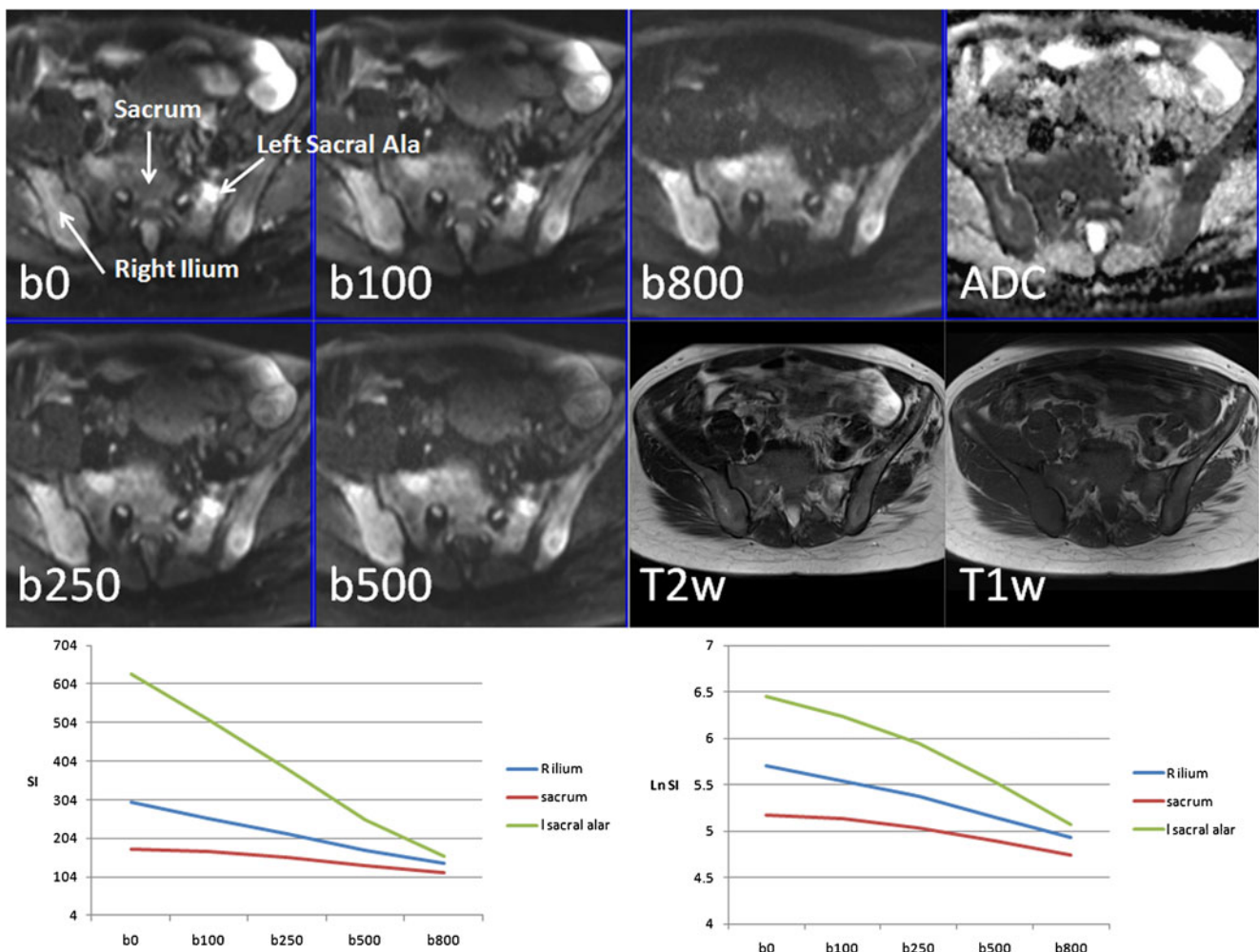


Fig. 1 Signal intensity changes with increasing b-values. A 29-year-old female with metastatic squamous cancer of the cervix. At a b-value of 0 s/mm^2 (i.e. no diffusion gradients), free water appears bright because of intrinsic T2-weighting of the sequence. At b-values of 100 s/mm^2 , mesenteric vessels and bowel loops exhibit signal attenuation (black-blood images), and lesion detection is improved. Increasing conspicuity of bony metastases with increasing b-value can be seen. ADC maps show increased values in the left sacral alar metastases consistent with necrosis. For other lesions, the ADC values of normal and abnormal

bone marrow are very similar, emphasising that bony metastasis detection is better on high b-value images compared to ADC maps. Changes in signal intensity (*left graph*) and \log_n signal intensity (*right graph*) are shown for three regions of interest. Only mono-exponential behaviour of signal decay is demonstrated for the regions of interest used. The gradient of \log_n signal intensity (LnSI) decay is the ADC value. The calculated ADC values for the three regions of interest are right ilium= $661 \mu\text{m}^2/\text{s}$, normal sacral bone marrow= $503 \mu\text{m}^2/\text{s}$ and left lytic sacral metastasis= $1,582 \mu\text{m}^2/\text{s}$

Currently, the most common way of acquiring DWI is via single shot echo planar imaging (SS-EPI) sequences which offer significantly faster acquisition times, thus overcoming DWI sensitivity to patient movement while still offering a relatively high SNR. A major limitation of DWI-EP imaging is susceptibility artefacts, particularly at tissue interfaces common in musculoskeletal imaging, such as air or bone and soft tissue, which can lead to severe geometric image distortion. Similarly, implanted metal work is another problematic source of artefact. As a result, SS-EPI may yield low image quality with low anatomic detail. Another inherent limitation of SS-EPI is the relatively low spatial resolution, which, owing to rapid T2* decay of signal, is

limited to matrix sizes of 128×128 . Recent advances in SS-EPI to overcome these problems include improved gradient systems with reduced eddy current effects which can help reduce geometric distortions and parallel imaging techniques employing multiple receiver coil elements to improve acquisition times and increase spatial resolution.

An alternative approach has been to acquire EPI data using a segmented or multi-shot, echo planar readout (MS-EPI), which divides the echo train into several shorter parts. This makes the image less sensitive to susceptibility artefacts, reduces image distortion and increases spatial resolution but at the price of longer acquisition times and therefore at a greater risk of motion artefact.

Diffusion-weighted single shot sequences based on the acquisition of spin echo trains have also been employed. Single shot fast spin echo (SS-FSE) and turbo spin echo (TSE) pulse sequences, also known as rapid acquisition with relaxation enhancement (RARE) or half-Fourier acquisition single-shot turbo spin echo (HASTE), are less sensitive to susceptibility artefact whilst maintaining the speed of EPI image acquisition time, albeit with a similar limited spatial resolution. Unfortunately, new image artefacts and longer echo time are consequences of this type of echo train readout scheme; to overcome them and maintain sufficient SNR often requires acquisition of multiple averages.

Steady-state free-precession (SSFP) sequences have also been used for DWI acquisition particularly for spinal pathology evaluations. The sequence type used is a PSIF sequence—a reverse of the acronym FISP (fast imaging with steady precession). This technique is quite different from those explained above, and the physics employed will not be discussed here in detail. However, it is important to be aware that the manner of diffusion-sensitisation employed does not allow easy determination of the diffusion-weighting b -value and therefore severely limits accurate ADC quantification. SSFP DWI yields only non-quantitative images using low equivalent b -values but has the advantage of short acquisition times to limit motion artefacts. Furthermore, the qualitative (visual) assessment of image contrast has proven valuable, particularly in the differentiation of vertebral collapse fracture aetiology as discussed below [3, 8, 9].

The DW data acquisition scheme continues to remain in development, and many investigators are exploring other methods of data acquisition that may enable many of the limitations mentioned above to be overcome [10]. Based on our own experience with the reliability and quality of images obtained, we recommend single shot EPI sequences for whole body diffusion MRI scans. Interested readers are directed to Table 1 where imaging parameters are given. In the future, it is hoped that agreed optimal imaging sequences and parameters for musculoskeletal imaging will eventually emerge.

Histologic correlates of diffusion-weighted imaging

The basic biological premise for the use of DWI is that malignant tissues are more cellular and have higher water content than benign/normal tissues; both these features will result in higher signal intensity of malignant disease on high b -value images with corresponding low ADC values. In addition, there are other microscopic organisational features that can affect tissue water diffusivity including tissue perfusion, cellular nuclear-cytoplasm ratio, distribu-

tion of cell sizes within a tissue, extracellular space tortuosity, integrity of cell membranes and the presence of necrosis.

In musculoskeletal imaging, a large focus of DWI has been on diagnostic and post-therapeutic assessment of malignant bone marrow infiltration. The literature suggests that ADC correlations with cellularity of the bone marrow are biphasic, with initial increases in high b -value signal intensity and ADC, as fat cells of yellow marrow are progressively replaced by normal red marrow elements and/or tumour cells [11, 12]. The lower signal intensity on high b -value images and lower ADC values of yellow marrow are likely to be related to (1) reduced water content and (2) the fact that larger sized fat cells may theoretically impede water movements to a greater extent than smaller hematopoietic cells (because of increased extracellular space tortuosity). However once all fat cells within bone marrow are replaced, then increasing bone marrow cellularity results in decreasing ADC values (but there are continued increases in signal intensity on high b -value images). Thus, it appears that signal intensity changes on high b -value images more faithfully reflect changes in cellularity compared to ADC values (Fig. 2).

Assessing diffusion-weighted images

Restriction of diffusion results in increased signal intensity on b -value images which allows for qualitative assessment by visual analysis of acquired images. This is clinically useful particularly in global assessment of disseminated tumour burden, especially for whole body diffusion MRI techniques (Fig. 3). Disease progression will result in new areas of abnormal signal intensity or changes in the extent, symmetry and intensities of abnormalities and vice versa (Fig. 4a).

There are a number of pitfalls in the visual analysis of high b -value images which are related to the fact that DW images reflect both the cellular as well as the water content of tissues. Thus, post-operative seromas and tissue oedema secondary to fracture, degenerative disease, and radiation treatment can all appear as high signal intensity on b -value images. Similar appearances can be seen when bone tumours are successfully treated, particularly when there has been massive liquefactive necrosis. Increased lesion/tissue signal intensity on high b -value images (with corresponding increased ADC values) results from increased water content and is termed “T2 shine-through” (Fig. 5). Therefore, to avoid misinterpretations arising from visual assessment of signal intensity, it is essential to correlate b -value findings with ADC maps as well as analysis of the morphological features from the associated conventional MR sequences (Table 2).

Table 1 Data acquisition parameters for single body parts and whole body DWI examinations

Machine parameters	Single body part imaging	Whole body imaging
Field of view	260 cm	380–400 cm
Matrix size	160–256	128i
TR	>3,500 ms	>6,000 ms; multiple stations as required to cover the body
TE	min	min
NSA	6	6
Fat suppression	SPAIR/STIR	STIR
EPI factor	114	47
Parallel imaging factor	2	2
Section thickness	5 mm/1 mm gap	5 mm/0 mm overlap
b-Values (s/mm ²)	0, 100, 800	0–50 and 800–1,000

Imaging parameters have been optimised for 1.5 T MR systems

TR Repetition time, TE echo time, NSA number of signal averages, SPAIR spectral selected attenuation inversion recovery, STIR short tau inversion recovery, EPI echo planar imaging, i interpolated

Analysis of ADC maps yielded from DWI allows for quantitative assessment of findings. Most studies report on single median or mean values of ADC using whole tumour regions of interest or selected areas within tumours. However, visual inspection shows that tumours are often heterogeneous in their spatial ADC distributions. Simple measures of central tendency have limited ability to detect treatment-related changes if there are both increases and decreases in ADC values. In these cases the net mean or median changes in ADC values are reduced, thus hiding treatment-related effects. It is possible to capture some aspects of displayed heterogeneity in the descriptors of histograms such as range, standard deviation, centile

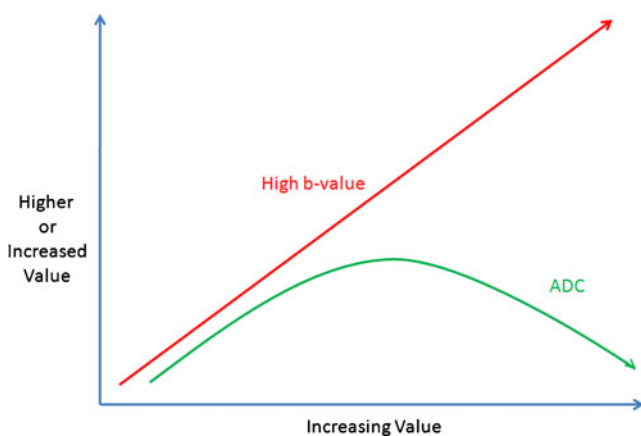


Fig. 2 Expected changes in signal intensity on high b-value images with increasing cellularity and water content of bone marrow. An abundance of fatty cells and low water content causes low signal intensity on high b-value images and low ADC values. Increasing bone marrow cellularity with replacement of fat cells and increases in water content cause an initial increase in signal intensity on both b-value images and ADC maps. Once fat cells are replaced, increasing cell density may cause lowering of ADC values, but persistent increases in signal intensity on high b-value images are seen

values, skewness, kurtosis and percentage of voxels above or below ADC cut-off values. Changes in histogram descriptors can then be correlated with change over time from disease progression or post-therapy response (Fig. 4b).

A new analytic method for retaining spatial information in response to therapy in bone is called the functional diffusion map (fDM) or the ADC parametric response map (PRM_{ADC}) [13]. This method requires that pre- and post-therapy ADC volumes are spatially registered using sophisticated software. Fortunately, rigid registration works well for bone disease. Differences in the registered voxel data between the two examinations are determined, and threshold values for ADC change are applied according to predetermined criteria. Changes in voxels are then colour labelled (such as red for increase, green for no change and blue for decrease) and overlaid onto anatomic images enabling the spatial distribution of changed voxels to be appreciated. This approach also allows for the quantification of the relative tumour volume in which changes have occurred. These statistical changes can then be correlated with therapy response in their own right [14].

Image display

There are a number of ways of displaying diffusion-weighted images. Inverted grey or arbitrary colour scales (so-called false-colour maps) are often used to visualise the data as sliced data or they can be stacked and viewed as multiplanar reconstructions and maximum intensity projections (MIP). Reader should note that although no colour scales are especially suited for the display of high b-value images, convention has it that inverted grey scales are used. It is also possible to fuse high b-value images with anatomic images using advanced software algorithms.

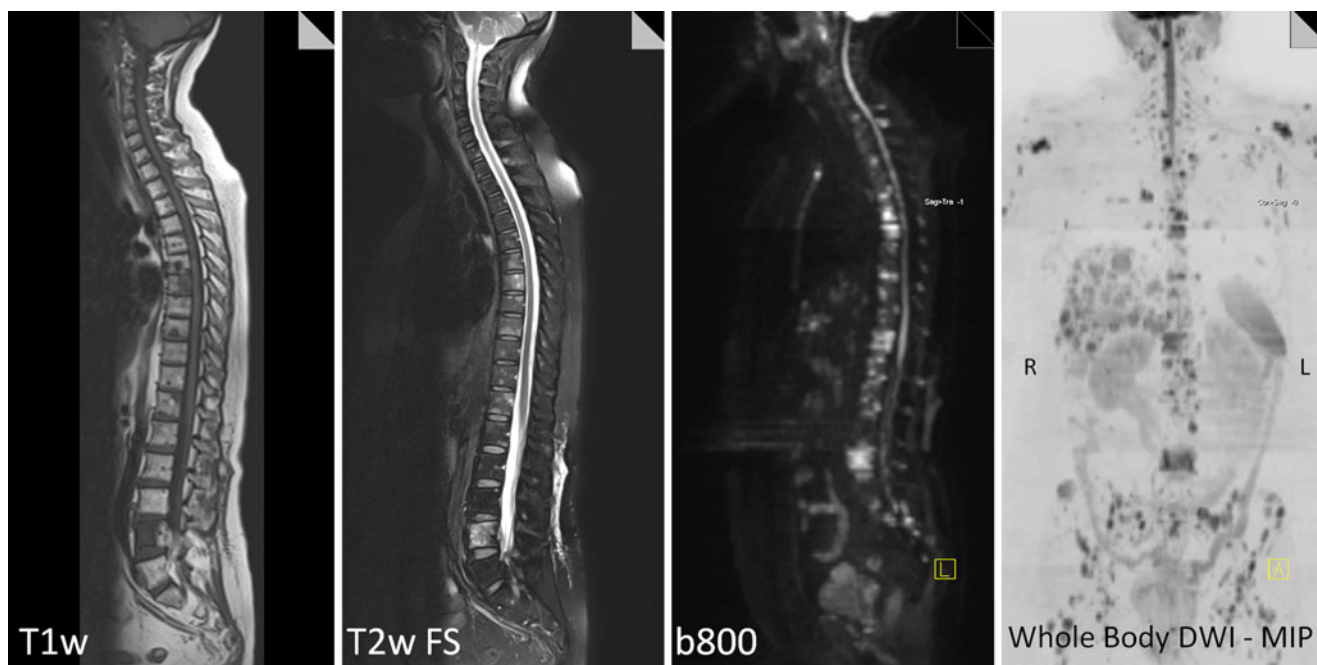


Fig. 3 Assessing whole body tumour burden with DWI. Diffuse bone metastases from primary breast carcinoma in a 27-year-old female patient. Vertebral body T1w hypointensity and hyperintensity on T2w-FS with corresponding high signal intensity on sagittal reconstructed

b-800 DW images. The whole body inverted grey-scale maximum intensity projection (MIP) image gives quick assessment of tumour distribution and volume including metastatic liver disease

Fusion of high b-value images with anatomic images has not been found to aid in lesion detection but appears to be helpful for lesion localisation [15]. Three-dimensional fusion imaging of high b-value DW-MRI with anatomic imaging has a number of uses including presenting data to clinicians, depicting and guiding biopsy to variable tumour cell sites in areas of scarring and aiding in CT volume determination for radiotherapy plans.

The concept of diffusion-weighted whole-body imaging with background body signal suppression (DWIBS) was introduced with a view to a new innovative technique to detect malignancy throughout the body in one imaging examination [16] (Figs. 3 and 4a). Such an approach has clear potential for the detection, staging and follow-up of malignancy. The ability to offer in one image a whole body assessment, drawing attention to all potential lesions, is attractive and reduces image interpretation time of whole-body MRI alone [17]. The majority of studies have focused on identifying the primary visceral tumour or lymph nodal metastases.

A recent study of the use of DWIBS specifically for the identification of bone metastases compared it to the traditional whole body investigation of bone scintigraphy [18]. Overall, the study demonstrated DWIBS as a technique comparable to bone scintigraphy for the detection of bone metastases, with an increased sensitivity only when there were more than 10 metastases.

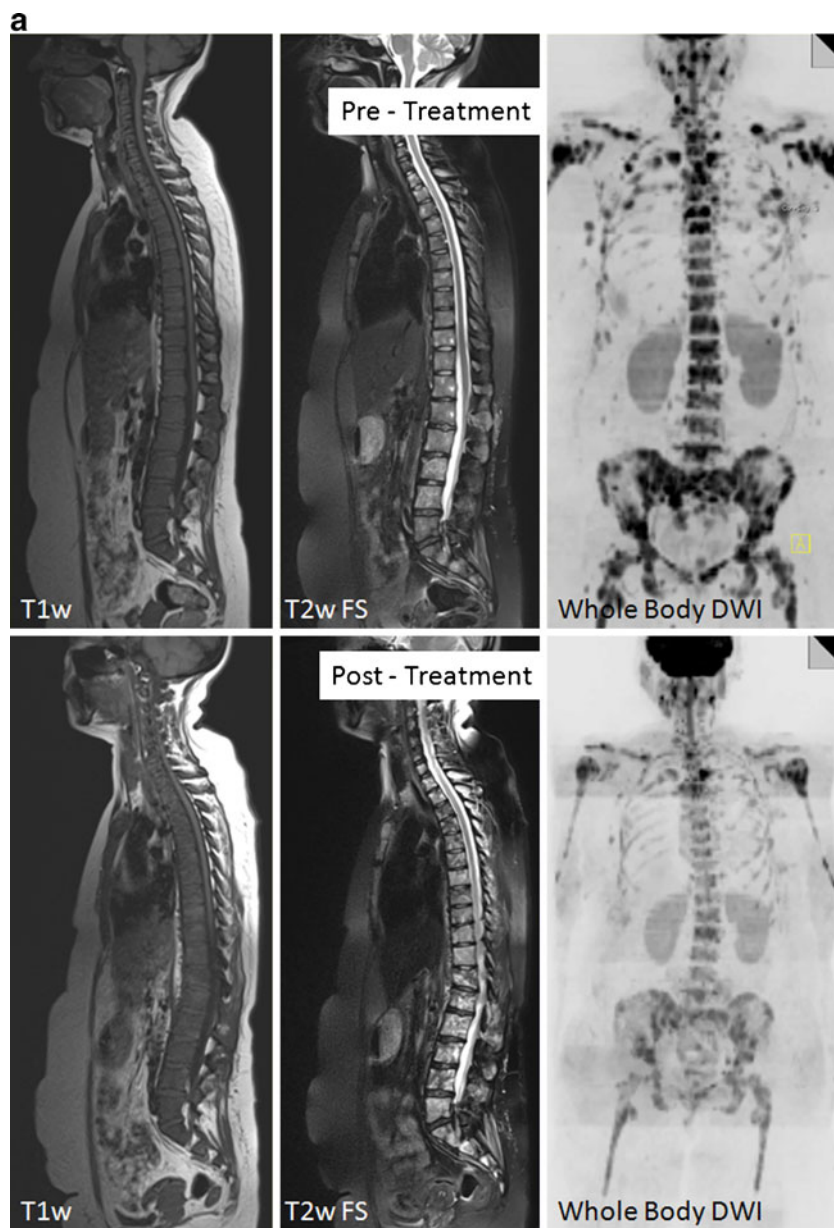
Clinical applications of DWI in musculoskeletal imaging

Vertebral fractures

DWI has been extensively evaluated for its role in the assessment of vertebral compression fractures, specifically for differentiating between benign and malignant causes. This is of great significance for subsequent patient management and prognosis. Assessments by conventional MR imaging require careful analysis of the morphology and pattern of bone marrow changes of the fracture, such as the presence of fracture lines, fluid clefts, involvement of the posterior elements, multiplicity of lesions and associated paravertebral soft tissues. However, there may be overlap of these appearances in both benign and malignant vertebral compression fractures, and it is often not possible to confidently distinguish these entities. Many radiologists use other sequences to aid in this distinction including susceptibility-weighted gradient-echo sequences, contrast enhancement and, more recently, DWI sequences.

The pathophysiological basis of diffusion changes in vertebral fractures is not fully understood, but the most agreed hypothesis is that, for an acute osteoporotic fracture, the resultant bone marrow oedema within bony trabeculae and microstructure disruption increase diffusion compared to the increased cellularity of tumour-related fractures, which causes restricted diffusion [3].

Fig. 4 a Metastatic breast cancer responding to chemotherapy. Disseminated bone metastases from triple negative breast carcinoma (37-year-old female) before and after 2 months of chemotherapy. The conventional T1w and T2w sequences do not demonstrate any significant signal intensity or morphological change to infer therapeutic progress (new wedge fracture of T12), but the whole body DWI inverted grey-scale MIP images conclusively demonstrate a significant decrease in signal intensity in multiple bone and subcutaneous metastatic deposits, suggestive of effective chemotherapeutic treatment. **b** Histogram analyses of ADC data. Top row shows representative images of a single infiltrated lumbar vertebral body showing increases in ADC values. ADC analysis of infiltrated lumbar vertebral bodies and whole pelvic skeleton from patient in **a** from pre-treatment (labelled “prior study” in *blue*) and post-treatment studies (labelled “current study” in *orange*). The histographic representation of ADC values clearly demonstrates an overall increase in ADC values subsequent to treatment, indicating tumour cell lysis in successful therapy. Mean ADC values of the two histograms are $924 \mu\text{m}^2/\text{s}$ (prior) and $1,900 \mu\text{m}^2/\text{s}$ (current). Data analysed using Oncotreat software (Siemens Healthcare)



First described by Baur [3], vertebral compression fractures can be differentiated on DWI by qualitative assessment of the signal characteristics, with benign osteoporotic fractures returning a hypo- or isointense signal compared to hyperintense signal from fractures secondary to tumour or metastases. Several studies have followed using a similar qualitative, non-quantitative assessment of DWI characteristics and have demonstrated similar positive findings [4, 19–21] (Figs. 3, 4a, 6a, b, 7a, b).

One study did not demonstrate any additional advantage of DWI in the characterisation of vertebral fractures [22], where some metastatic collapse fractures were hypointense at a single b-value of $165 \text{ s}/\text{mm}^2$. However, it has been argued that the pathologies investigated in this study

included sclerotic metastases, which appear hypointense on multiple MR sequences including DWI due to their low water content, and metastases that had been treated with radiotherapy [23, 24]. Similar false-negative results of DWI hypointensity with sclerotic metastases have been demonstrated in other studies [4, 25]. The presence of vertebral sclerotic metastases in the clinical situation are less problematic than lytic metastases, which are more likely to cause vertebral collapse, cord compression and tumour pain. Equally, the appearance of sclerotic bone following treatment, be it radiation, chemotherapy or bisphosphonates, is often considered a sign of treatment success with the sclerotic matrix more likely to prevent skeletal adverse events than lytic tumour tissue. Nonetheless, it highlights

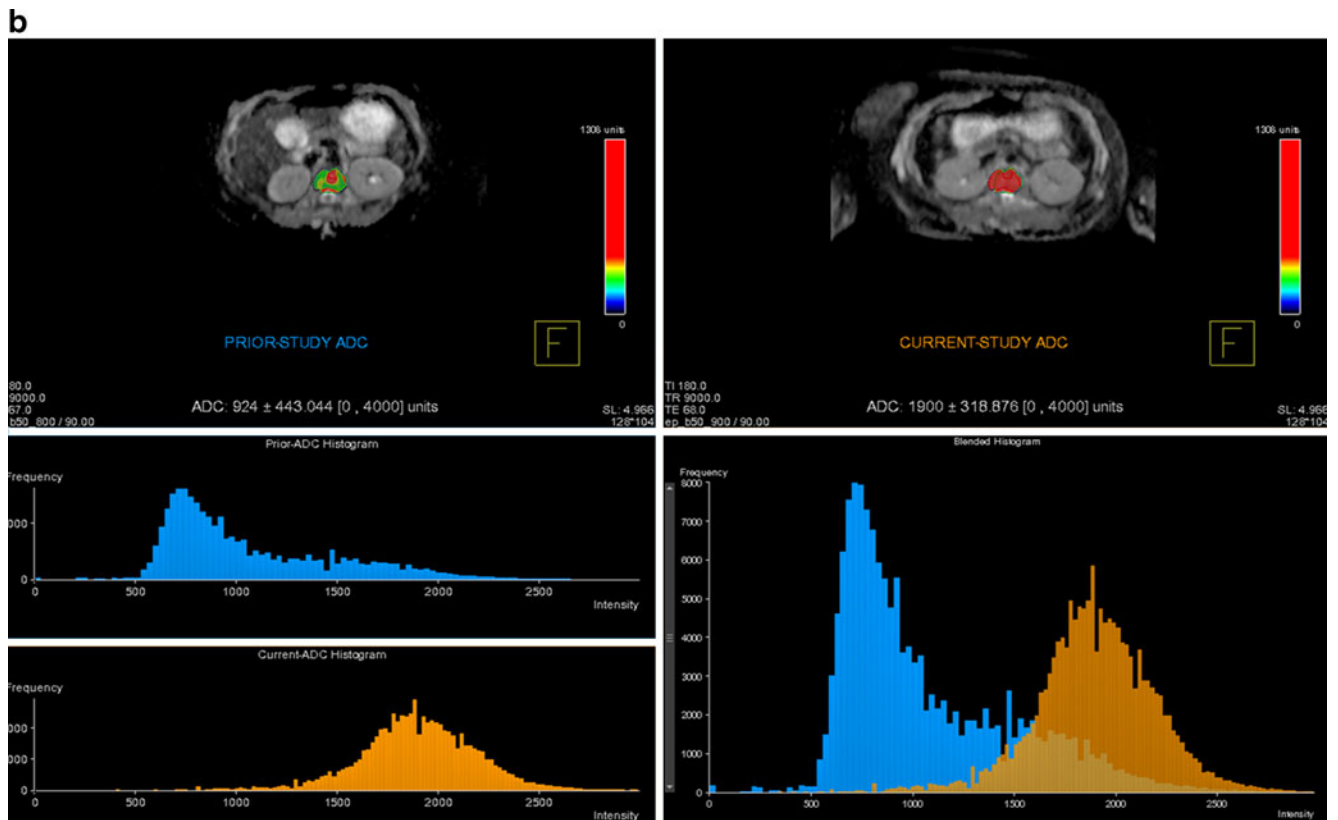


Fig. 4 (continued)

Fig. 5 T2 shine through. Post-radiotherapy pelvic axial images of a 75-year-old male patient with metastatic oesophageal carcinoma. There is a large left iliac metastatic deposit (*arrows*) demonstrating high signal on the b800 image, which could suggest restricted diffusion and residual metastatic tumour tissue. However, on the ADC map, there are increased ADC values of the same lesion, indicating high free water content. The combination of high lesion signal on b-value and high ADC images is termed “T2 shine through”

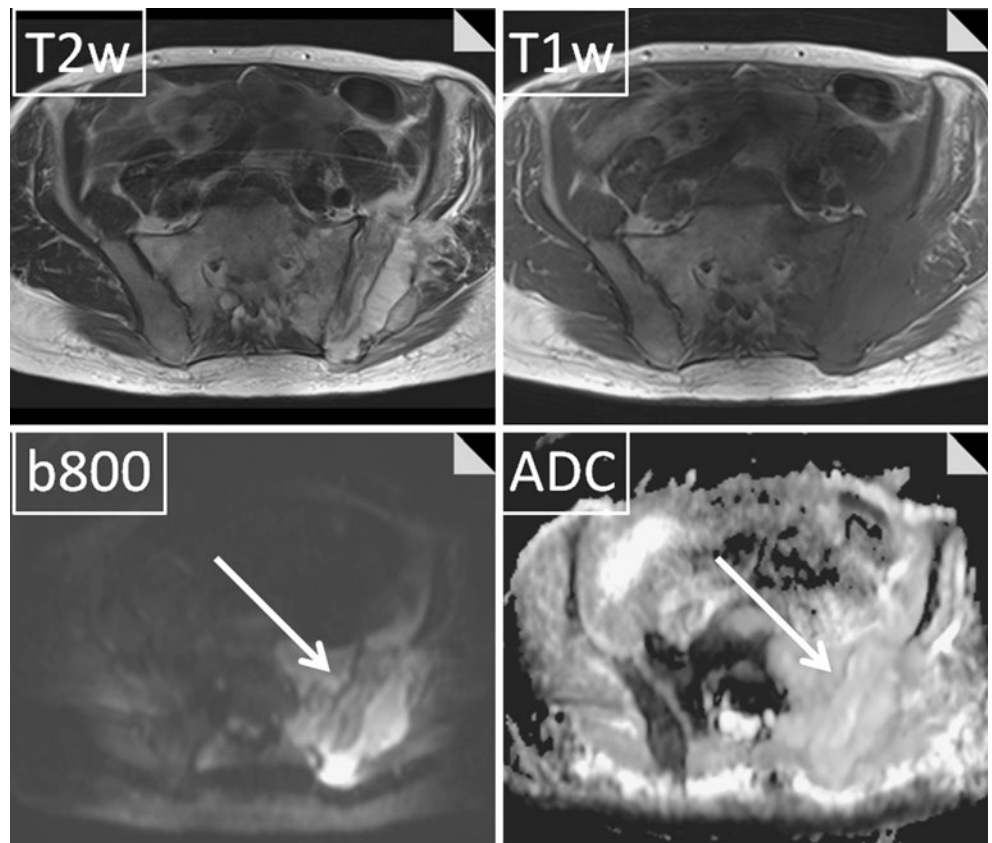


Table 2 Image interpretation guidelines for DWI

Signal intensity on high b-value images	ADC maps	Interpretation
↑	↓	Generally, high cellularity tumour; rarely abscess, viscous fluids or blood products
↑	↑	T2-shine through; Liquefactive necrosis
↓	↑	Fluid; Necrosis; Lower cellularity; Tumours with gland formation
↓	↓	Fibromuscular issues. Fat.
	↔	Mature fibrous tissue with low water content

that DWI should not be interpreted in isolation but in conjunction with other imaging modalities or sequences that are able to detect sclerotic bone, to avoid the pitfalls of false negatives in sclerotic states.

Quantitative analysis of DWI can be achieved by analysing the ADC in a region of interest within the abnormal vertebral body. Using similar patients as in the above studies, it has been shown that the ADC values do correlate with the qualitative DWI findings in that non-metastatic fractures have a higher ADC value when compared to the low ADC values of metastatic fractures [4, 8, 21, 26]. However, there is considerable variability in the ranges of ADC values, to the point of overlap in both patient groups, which is thought to be related to different DWI pulse sequences and diffusion gradients used (Table 3), but may also additionally be due to the biphasic alteration in ADC with the degree of metastatic infiltration, although the histologic reality is unlikely as vertebral body collapse should only occur once all the normal bone marrow has been replaced. As a result, no threshold differentiating ADC value can be determined and clinically applied at present.

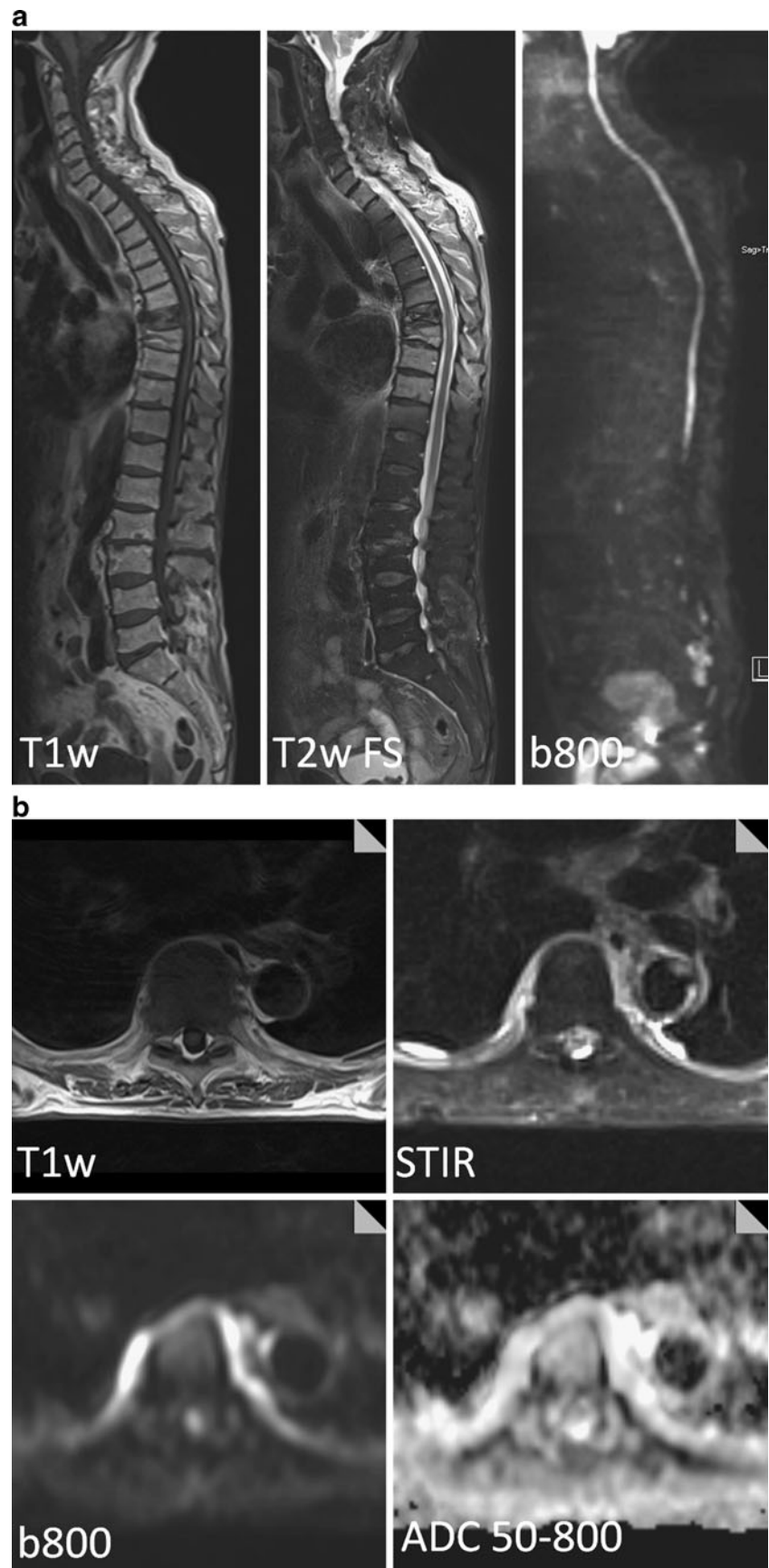
Of the multiple studies assessing the value of marrow DWI signal in vertebral fractures, the largest study group had 82 patients, with a total of 102 vertebral fractures [27]. For this particular study, the resulting sensitivity, specificity, positive predictive value (PPV) and negative predictive value (NPV) were 100, 93, 91 and 100% respectively. Several similar studies have not quoted sensitivity or specificity values, preferring to use quantitative results regarding the proportion of hypo-, iso- and hyperintense DWI signal returned by vertebral body marrow for benign or malignant fracture aetiology. However, of those studies that have, many have returned similarly high sensitivities and specificities above 85% [3, 20, 28], but there has been some variability with quoted sensitivities being as low as 42% in a 46 patient study [29].

By comparison, older studies defining the ability of conventional MR sequences of T1w, T2w and STIR images to differentiate between benign and malignant vertebral compression fractures have yielded sensitivities and specificities of 85–100% and 79–100% [30–33]. The morphological changes associated with each pathology demonstrated by conventional MR imaging have yielded high predictive values with 100% PPV for an osteoporotic vertebral fracture in the presence of a retropulsed fragment but lacking an epidural mass or abnormal pedicle signal intensity, whereas the presence of an associated epidural soft tissue mass has a 100% PPV for a malignant aetiology [34].

Clearly, studies are required to define the true additional effectiveness and accuracy of DWI over conventional sequences in problematic patients where conventional MR images have yielded equivocal findings. At present, there have been no such studies concentrating solely on vertebral fractures deemed equivocal by MR findings, but it has been noted that the original diagnoses made on routine MR sequences, including one such equivocal patient where it was not possible to differentiate between a benign or malignant aetiology, have been subsequently changed due to the DWI findings [20], thereby possibly giving an indication of a genuine true additional value of additional DWI sequences.

The studies reviewed seem to indicate that there is some added value for performing DWI to assist in the differentiation between benign or malignant aetiologies of vertebral compression fractures. However, DWI does have limitations in that it is clearly not suitable for sclerotic fractures and, consequently, sclerotic treated metastases, where inadvertent diffusion imaging without appropriate clinical details or plain radiographs could lead to false-negative results. A lesser discussed finding is that of false-positive DWI hyperintensity in benign fractures, which can be

Fig. 6a, b Non-malignant T7 vertebral collapse in an osteoporotic patient. Sagittal T1w, T2w with FS and b800 DWI spine images. The T7 vertebral collapse has the morphological appearance of a metastasis, but there is total absence of restriction of diffusion (no signal intensity increase on high b-value images) within the collapsed vertebral body on **a** the sagittal images or **b** small field of view axial images, suggestive of a non-malignant aetiology. The axial conventional spin echo and diffusion-weighted b-800 and ADC images demonstrate high paravertebral signal intensity in keeping with a paravertebral haematoma. Care should be taken however to analyse other image modalities as sclerotic metastases do not demonstrate any significant hyperintensity on diffusion-weighted images



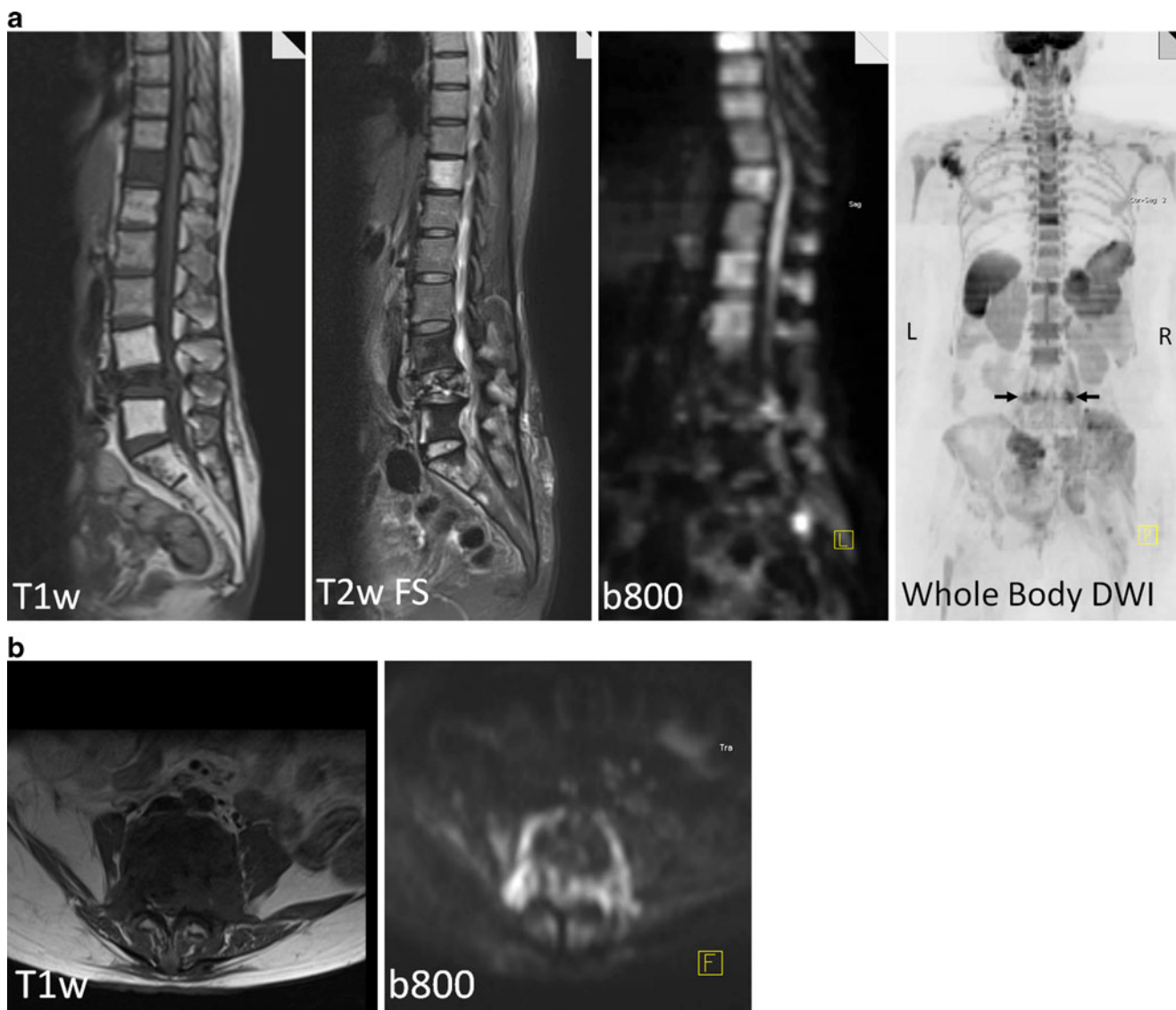


Fig. 7a, b Benign vertebral body collapse with paravertebral tumour tissue. Sagittal T1w, T2w-FS, b800 and inverted whole body DWI image (**a**) of a patient with disseminated metastatic breast cancer. Previous spinal irradiation of L3–L5. There is collapse and signal abnormality on the conventional T1w and T2w imaging of the T11 and L4 vertebral bodies, but it is not possible to confidently define whether there is active disease present at L4. On corresponding DWI, there is absence of high signal intensity within the collapsed L4

vertebral body, but L4 paravertebral restricted diffusion is seen on whole body b800 image (posterior projection; *black arrows*). Axial T1w and b800 DWI through L4 body (**b**) demonstrate high SI on high b-value images consistent with impeded water diffusion in paraspinal soft tissue mass but no evidence of residual tumour within collapsed vertebral body. Note the multi-level spinal metastatic disease elsewhere on whole body imaging. Images of the right hemipelvis are distorted due to the placement of a dynamic hip screw

attributed to extensive oedema or haemorrhage [27]. Confident diagnosis in this situation requires correlations with conventional MRI sequences and with sequences which depict the intactness of bony trabeculae [susceptibility-weighted gradient echo sequences and ultrashort echo (UTE) sequences] or alternatively CT scan appearances (Fig. 6a, b). ADC values may occasionally be helpful for additional differentiation between benign and malignant compression fractures particularly if ADC values are markedly raised but, in view of the variability of measured values and lack of a defined threshold differentiating ADC

value, quantitative diffusion analysis cannot consistently provide definitive diagnosis when used in isolation.

Other bone marrow abnormalities

The assessment of bone marrow changes extends beyond differentiating the causes of vertebral compression fractures to include other bone marrow pathology, including infection and haematological malignancies, and determining the extent of metastases and their response to treatment.

Table 3 Quantitative DWI of vertebral bone marrow with fractures and metastases

Pulse sequence type	Study	b-Values (s/mm ³)	Apparent diffusion coefficient (10 ⁻³ mm ² /s)		
			Benign (osteoporotic/ traumatic) fracture	Malignant fracture (mf) or metastasis (m)	Normal vertebral bone marrow
SS-EPI	Chan et al. 2002 [25]	200–1,000	1.94±0.35	0.82±0.0 (mf)	0.23±0.05
	Ballon et al. 2004 [57]	0, 1,000	–	0.70±0.21 (m)	–
	Pui et al. 2005 [26]	0–1,000	–	1.02±0.36 (m)	0.30±0.21
	Oner et al. 2007 [58]	0, 600	1.61±0.46	0.72±0.31 (m)	0.53±0.15
	Tang et al. 2007 [59]	0, 300	2.23±0.21	1.04±0.03 (mf)	–
SS-FSE	Zhou et al. 2002 [60]	0, 150, 250	0.32±0.05	0.19±0.03 (m)	0.27–0.35
	Oner et al. 2007 [58]	0, 600	1.54±0.36	0.69±0.30 (m)	0.36±0.15
	Raya et al. 2007 [61]	0–750	1.25±0.26	0.97±0.14 (m)	0.21±0.06
MS-EPI	Herneth et al. 2000 [62]	0, 440, 880	0.86	0.39±0.11 (m)	1.13±0.23
	Herneth et al. 2002 [63]	440, 880	1.61±0.37	0.71±0.27 (mf)	1.66±0.38
	Balliu et al. 2009 [64]	0, 500	1.90±0.39	0.92±0.13 (m)	–
SSFP-DWI	Byun et al. 2007	0, 650	0.88±0.07	0.78±0.03 (mf)	0.21±0.06
Typical values			1.0–2.0	0.7–1.0	0.2–0.6

SS-EPI Diffusion-weighted single-shot spin-echo echo-planar imaging sequence with fat saturation, *MS-EPI* diffusion-weighted multi-shot (segmented) spin-echo echo-planar imaging sequence with fat saturation, *SSFP-DWI* steady-state free precession diffusion-weighted sequence

Bone marrow infection

While benign in nature, osteomyelitis can cause hyperintensity on DWI with resulting low ADC values, which may mimic malignancy [25, 26]. There is anecdotal evidence that early acute or particularly aggressive osteomyelitis may give rise to increased diffusivity resulting in hyperintensity on DWI and making it indistinguishable from malignancy [35]. These observations are related to the fact that protein-rich fluids are high in their viscosity and are therefore effective at impeding the free movement of water. The same effects are seen in endometriotic cysts and in abscesses. Thus, both tuberculous spondylitis [36] and pyogenic spondylodiscitis [26] have both been reported to demonstrate restricted patterns of diffusion. Thus, there is only limited value in using DWI to differentiate between infectious and malignant vertebral lesions, with approximately 60% sensitivity, specificity and accuracy [26]. As a result, DWI in this clinical situation cannot be recommended as a worthwhile additional diagnostic sequence at present.

Haematological malignancy of bone marrow

Assessment of bony involvement of malignant lymphoma by various MR sequences with histopathological correlation demonstrated a pattern of restricted diffusion in bone lymphoma on DWI [37]. This study showed that the specificity and sensitivity of DWI in the diagnosis of lymphoma were comparable with those of STIR images and

were slightly higher than T1-weighted spin-echo images. However, overall, it was concluded that whilst DWI is as useful as the more traditionally and widely used STIR sequences, the limitations in terms of resolution, artefacts and distortion from their particular DWI pulse sequence (echo planar) led to poorer quality images. As a result, the conclusion of this study was that a combination of T1-weighted and STIR images currently remains the most accurate assessment of bone lymphoma.

The conclusions of the above study do not take into account the fact that diffusion-weighted whole body imaging with background signal suppression (DWIBS) is ideally suited for evaluating the extent of both the bony and nodal extent of malignant lymphoma [38]. This method of assessment is practically useful and clinically appealing for both radiologists and referring physicians because it enables “at a glance” assessments of disease burden and distribution (staging) including changes with therapy (Fig. 4a). Disease progression on high b-value images is displayed as new areas of abnormal signal intensity or as changes in the extent, symmetry and intensity of abnormalities. With successful treatment, cell killing results in lowering of signal intensity. The physiological reasons for changes in bone marrow signal intensity with respect to the therapy are discussed in detail below in the next section.

Post-treatment follow-up of bone marrow changes

When bone marrow disease is treated successfully, the tumour cell death results in increased water diffusivity

manifested as increased ADC values. The signal intensity changes on high b-value images of responding metastatic bone marrow are more variable (initial increases or decreases); they can be patchy and difficult to interpret requiring serial follow-up in order to appreciate the time course of changes. In general there is a long-term decrease in the signal intensity of bony infiltrations accompanied by decreases in ADC values in the setting of successful therapy. Tumour necrosis, removal of apoptotic tumour cells, bone sclerosis, re-emergence of yellow marrow, loss of tissue water and secondary myelofibrosis assist in long-term reductions in signal intensity on high b-value images and in ADC values of successfully treated lesions. These DWI-depicted changes in water diffusivity can occur slowly, becoming visible many months after starting therapy, depending on the tumour type and type of therapy administered.

Changes in tissue diffusivity depicted by DWI can demonstrate and differentiate between viable tumour versus necrotic tissue during active treatment [4]. DWI of patients with leukaemia has showed marked increase in ADC values and increased diffusivity in areas of necrotic tissue which suggest successful treatment [39]. A recent study evaluating DWI monitoring of treatment response of vertebral metastatic deposits showed convincing changes from pre-chemotherapy b-value hyperintensity to hypointensity following therapy [4]. This study compared DWI with conventional spin-echo imaging. The T1W and T2W spin-echo follow-up images of spinal metastases revealed no significant interval changes—indicating that they are of limited use in monitoring response to therapy. However, in patients with clinical improvement, the corresponding b-values showed demonstrable conversion to hypointensity on subsequent follow-up DWI at the end of therapy consistent with increased water molecular diffusion, secondary to cellular membrane loss from tumour cell apoptosis (i.e. successful treatment) (Fig. 4a, b). Equally, patients with no clinical improvement demonstrated persistent bone marrow b-value hyperintensity suggestive of persistent tumour hypercellularity causing persistent restriction of water diffusion. The clear clinical value of DWI over and above that achieved by conventional T1w and T2w spin echo sequences perhaps best highlights the advantages of adding DWI sequences to routine protocols which many specialist oncology centres have now adopted.

It should be noted that there are pitfalls in the use of signal intensity alone to assess therapy response within malignant bone marrow. Occasionally, massive liquefactive necrosis occurs [as opposed to programmed cell death (apoptosis)] in response to successful treatment. This has been noted particularly in patients with multiple myeloma, lymphoma and occasionally in other solid metastatic neoplasms. In these cases, persistent high signal intensity is

observed on high b-value images with high ADC values (T2 shine through) which can last for years. This emphasises the need to always interpret DWI with ADC maps and conventional sequences in order to accurately make determinations regarding therapy responsiveness.

Primary soft tissue tumours

Soft tissue tumours often have overlapping MRI appearances that preclude confident diagnosis without biopsy. DWI has yielded only moderate diagnostic success in soft tissue tumour characterisations. Early studies showed that the mean ADC values between malignant and benign tumours were not significantly different and demonstrated extensive overlap [40–43]. This is thought to be due to the high heterogeneity and variability of composition of soft tissue tumours, as demonstrated by increased ADC values of myxoid tumours when compared to non-myxoid tumours, reflecting the high mucin and low collagen content of a largely fluid tumour [42, 43]. For non-myxoid tumours, malignant masses have a significantly lower ADC value than benign tumours in the non-myxoid group, but overall the marked overlap between benign and malignant soft tissue masses has led authors to conclude that DWI cannot be used alone to characterise soft tissue masses.

A more recent small study has shown that DWI could be used to differentiate between sarcomas and chronic expanding haematomas, a rare and gradually enlarging lesion that may be misdiagnosed as a haemorrhagic malignant soft tissue mass due to its size and progression [44]. Chronic expanding haematomas can have similar appearances to haemorrhagic soft tissue sarcomas, but due to their low cellularity, they have a significantly higher ADC value than a malignant mass on DWI [44]. However, the small number of patients within this study (34 patients, of which only 6 had chronic expanding haematomas) together with the assessment of a single soft tissue entity has not greatly advanced the use of DWI for general soft tissue mass evaluation.

DWI differentiation of post-therapeutic change and recurrence of soft tissue tumours has also been explored. In soft tissue sarcomas treated with chemotherapy, increases in ADC values are associated with reductions in tumour size and vice versa; as a result, strong negative correlations between tumour volume and ADC changes have been reported ($r=-0.925$, $P<0.0001$) [45]. However, the post-therapeutic changes in soft tissue tumours can be difficult to differentiate from early recurrence due to the similar high T2w and STIR signal with corresponding low T1w signal [46]. The higher DWI signal loss (hypointensity) of post-treatment seromas and muscle oedema was shown to be

significantly different from that of viable recurrent tumour [46]. However, studies evaluating DWI of primary soft tissue tumours [40–43] have shown high degrees of variability and overlap in the b-value qualitative appearances and quantitative ADC values of benign and malignant soft tissue tumours such that DWI findings may not be applicable to all the different histological types of soft tissue tumours.

Primary bone tumours

Plain radiography and conventional MRI are typically used in imaging of primary bone tumours for lesion characterisation and local staging, while distant staging for high-grade sarcomas is performed with a combination of chest CT and whole body bone scintigraphy. In the majority of cases, the combination of radiography and MRI is highly successful in lesion characterisation and deciding whether needle biopsy is required prior to further management.

One area of potential difficulty that has been extensively investigated is the differentiation between large chondromas and low-grade chondrosarcomas [47]. However, this only becomes relevant if there is a difference in management between the two conditions. Both entities are classed as clinically low-grade tumours (as opposed to grade 2 and 3 chondrosarcoma and dedifferentiated chondrosarcoma, which are classed as clinically high-grade tumours) and can be successfully treated with intralesional curettage. A study utilising DWI to differentiate chondrosarcomas from benign bone tumours did not demonstrate any significant difference in the qualitative and quantitative DWI appearances with significant overlap between different pathologies [48]. Whilst simple bone cysts did demonstrate significantly higher ADC values, similar to the study findings regarding soft tissue tumours, a positive finding for a single pathological entity is of limited clinical value. Therefore, at present, there does not appear to be a role for DWI in the characterisation or local staging of primary bone tumours.

However, the potential of whole body DWI for distant staging needs to be investigated. Currently, ^{99m}Tc MDP whole body bone scintigraphy is routinely used for assessment of skeletal metastases in the setting of primary high-grade bone sarcomas such as osteosarcoma and Ewing sarcoma. With Ewing sarcoma in particular, the poorer sensitivity of identifying metastatic bone marrow infiltration on scintigraphy, when compared to MRI and positron emission tomography (PET) using fluorine-18 fluorodeoxyglucose (FDG-PET) is a recognised problem [49, 50]. This may be overcome to some extent by the use of whole body MRI with whole body diffusion sequences, recognising that in the young patient population affected by this condition, the differentiation between pathological marrow infiltration

and hyperplastic red marrow may be problematic for some patients.

Recent literature has shown value in DWI for assessment of post-therapeutic response in primary bone tumours such as osteogenic and Ewing's sarcoma. Assessment of osteosarcoma response to neo-adjuvant chemotherapy by conventional MRI is problematic as the tumour does not significantly reduce in size and may even show apparent increase in size, possibly due to visualisation of surrounding connective tissue, ossification and oedematous changes. Equally, there is little change in the mineralised matrix components of the tumour whilst the remainder of the tumour can demonstrate non-specific signal changes. Successful chemotherapeutic response is classed as >90% tumour necrosis on histology [51], and it has been postulated that this can be quantitatively assessed by DWI. Mean ADC values have been shown to increase correspondingly with increases in tumour necrosis, as defined by macroscopic tumour evaluation. Several studies have shown that there are significant differences in ADC values between patients who responded to treatment (and had higher ADC tumour values) and those who were non-responsive [52–54]. The clear value of the ability of DWI to highlight post-therapeutic responders versus non-responders is particularly pertinent as the tumour volumes were not shown to be significantly different between the two groups [54].

Interestingly, one study evaluated both the minimum and mean ADC values in patients with treated osteosarcomas examined with EPI-DWI with b-values of 0 and 1,000 [55]. Both values were significantly increased following treatment when compared to pre-treatment ADC values. However, when the patients were categorised into those with histologically successful treatment (i.e. >90% tumour necrosis) and those with <90% tumour necrosis, only the minimum ADC value was significantly different between the two groups [55]. The average ADC values of the tumours were not significantly different between these groups, and it was suggested that the discrepancy between minimum and mean ADC changes may reflect the post-treatment cellular heterogeneity of treated tumours. Thus, single median or mean values of ADC may not capture treatment-related changes if both increases and decreases in ADC values are seen, thus hiding treatment-related effects. In regard to this study, the authors suggested that areas of highest cellularity within a tumour mass should best reflect the characteristic of residual viable tumour tissue, and thus the minimum ADC value which reflects such hypercellularity may therefore provide the best prognostic post-therapeutic assessment.

A further area of potential difficulty in post-chemotherapy MR assessment of high-grade bone sarcomas is the effect of granulocyte colony stimulating factor (G-CSF). The resulting

marrow hyperplasia can mimic tumour extension on conventional T1w spin-echo sequences. G-CSF administration during chemotherapy treatment (for the moderation of neutropenia occurring during treatment) can be a potential pitfall on high b-value DWI, where it results in increased bone marrow signal intensity but without disease progression. This is due to increased bone marrow cellularity resulting from G-CSF for the production of white blood cells. The effects on bone marrow signal can occur within 2 weeks of the first G-CSF dose [56], but it is unclear whether additional doses further alter bone marrow signal intensity or whether there is resolution of changes on cessation of therapy. It is therefore challenging to confidently differentiate between pathological bone marrow infiltrations from the benign red marrow reversion changes, but disease progression can be suspected in new areas of focal abnormal signal intensity or by changes in the extent, symmetry and intensity of pre-existing abnormalities, in conjunction with correlation with ADC values and morphologic MR appearances. On the other hand, G-CSF-induced bone marrow hyperplasia increases signal intensity in normal adult red marrow areas (spine, vertebrae, pelvis, sternum, ribs) with reversion of yellow marrow to red marrow also seen in the proximal limb bones.

Conclusions

There have been recent advances in the techniques and applications of DWI for the investigation of musculoskeletal pathologies. While the availability of DWI has also become more widespread, the relative value of DWI sequences in addition to or as alternatives to conventional MR sequences is equivocal for many conditions.

There is no doubt that DWI is a sensitive tool in the assessment of bone marrow, with greatest success in the differentiation between benign and malignant vertebral compression fractures. However, there is often significant overlap in the resultant qualitative and quantitative findings, and it is also important to be aware of DWI's limitations in assessing sclerotic bone metastases in particular. Nonetheless, there is clear data to suggest that, for equivocal vertebral fracture cases, additional DWI data can add to diagnostic confidence.

Follow-up of post-treatment spinal metastases by DWI has shown equally promising results where conventional T1w and T2w sequences have limited value. DWI's ability to differentiate between areas of cell necrosis from treatment with high diffusivity versus highly cellular residual tumour tissue with restricted diffusion has clear clinical value, and its use has been adopted widely at specialist oncology centres. Most recently, whole body staging for bone metastases by DWIBS has been demonstrated to be as effective as bone

scintigraphy but without the associated radiation burden. DWI also has obvious advantages as a non-invasive, non-ionising MR technique that is quick to perform and requires no injection of contrast medium.

Allowing for the relative paucity of available literature in this area, an overlapping spectrum of diagnostic DWI findings between benign and malignant aetiologies has been found when assessing soft tissue tumours, bone tumours and bone infection, which limits its clinical value in this regard.

Our review shows that DWI has potential value in selected patient groups. At present, DWI appears to only add slightly to the overall diagnostic yield of conventional sequences particularly in lesion characterisation, and it is only in certain clinical conditions that it has true discriminatory value. Musculoskeletal radiologists are encouraged to consider its inclusion in clinical MRI protocols in selected patients.

Financial disclosure The authors have nothing to declare.

References

- Schaefer PW, Copen WA, Lev MH, Gonzalez RG. Diffusion-weighted imaging in acute stroke. *Magn Reson Imaging Clin N Am*. 2006;14(2):141–68.
- Karaarslan E, Arslan A. Diffusion weighted MR imaging in non-infarct lesions of the brain. *Eur J Radiol*. 2008;65(3):402–16.
- Baur A, Stähler A, Brüning R, Bartl R, Krödel A, Reiser M, et al. Diffusion-weighted MR imaging of bone marrow: differentiation of benign versus pathologic compression fractures. *Radiology*. 1998;207(2):349–56.
- Byun WM, Shin SO, Chang Y, Lee SJ, Finsterbusch J, Frahm J. Diffusion-weighted MR imaging of metastatic disease of the spine: assessment of response to therapy. *AJNR Am J Neuroradiol*. 2002;23(6):906–12.
- Bley TA, Wieben O, Uhl M. Diffusion-weighted MR imaging in musculoskeletal radiology: applications in trauma, tumors, and inflammation. *Magn Reson Imaging Clin N Am*. 2009;17(2):263–75.
- Turner R, Le Bihan D, Maier J, Vavrek R, Hedges LK, Pekar J. Echo-planar imaging of intravoxel incoherent motion. *Radiology*. 1990;177(2):407–14.
- Le Bihan D, Turner R, Douek P, Patronas N. Diffusion MR imaging: clinical applications. *AJR Am J Roentgenol*. 1992;159(3):591–9.
- Raya JG, Dietrich O, Reiser MF, Baur-Melnyk A. Methods and applications of diffusion imaging of vertebral bone marrow. *J Magn Reson Imaging*. 2006;24(6):1207–20.
- Karchevsky M, Babb JS, Schweitzer ME. Can diffusion-weighted imaging be used to differentiate benign from pathologic fractures? A meta-analysis. *Skeletal Radiol*. 2008;37(9):791–5.
- Padhani AR, Liu G, Koh DM, Chenevert TL, Thoeny HC, Takahara T, et al. Diffusion-weighted magnetic resonance imaging as a cancer biomarker: consensus and recommendations. *Neoplasia*. 2009;11(2):102–25.
- Nonomura Y, Yasumoto M, Yoshimura R, Haraguchi K, Ito S, Akashi T, et al. Relationship between bone marrow cellularity and apparent diffusion coefficient. *J Magn Reson Imaging*. 2001;13(5):757–60.

12. Tang GY, Lv ZW, Tang RB, Liu Y, Peng YF, Li W, et al. Evaluation of MR spectroscopy and diffusion-weighted MRI in detecting bone marrow changes in postmenopausal women with osteoporosis. *Clin Radiol*. 2010;65(5):377–81.
13. Galbán CJ, Chenevert TL, Meyer CR, Tsien C, Lawrence TS, Hamstra DA, et al. The parametric response map is an imaging biomarker for early cancer treatment outcome. *Nat Med*. 2009;15(5):572–6.
14. Reischauer C, Froehlich JM, Koh D, Graf N, Padevit C, John H, et al. Bone metastases from prostate cancer: assessing treatment response by using diffusion-weighted imaging and functional diffusion maps—initial observations. *Radiology*. 2010;257(2):523–31.
15. Fischer MA, Nanz D, Hany T, Reiner CS, Stolzmann P, Donati OF, et al. Diagnostic accuracy of whole-body MRI/DWI image fusion for detection of malignant tumours: a comparison with PET/CT. *Eur Radiol* [Epub ahead of print]. doi:10.1007/s00330-010-1929-x
16. Takahara T, Imai Y, Yamashita T, Yasuda S, Nasu S, Van Cauteren M. Diffusion weighted whole body imaging with background body signal suppression (DWIBS): technical improvement using free breathing, STIR and high resolution 3D display. *Radiat Med*. 2004;22(4):275–82.
17. Kwee TC, Takahara T, Ochiai R, Katahira K, Van Cauteren M, Imai Y, et al. Whole-body diffusion-weighted magnetic resonance imaging. *Eur J Radiol*. 2009;70(3):409–17.
18. Gutzeit A, Doert A, Froehlich JM, Eckhardt BP, Meili A, Scherr P, et al. Comparison of diffusion-weighted whole body MRI and skeletal scintigraphy for the detection of bone metastases in patients with prostate or breast carcinoma. *Skeletal Radiol*. 2010;39(4):333–43.
19. Baur A, Huber A, Ertl-Wagner B, Dürr R, Zysk S, Arbogast S, et al. Diagnostic value of increased diffusion weighting of a steady-state free precession sequence for differentiating acute benign osteoporotic fractures from pathologic vertebral compression fractures. *AJNR Am J Neuroradiol*. 2001;22(2):366–72.
20. Spuentrup E, Buecker A, Adam G, van Vaals JJ, Guenther RW. Diffusion-weighted MR imaging for differentiation of benign fracture edema and tumor infiltration of the vertebral body. *Am J Roentgenol*. 2001;176(2):351–8.
21. Byun WM, Jang HW, Kim SW, Jang SH, Ahn SH, Ahn MW. Diffusion-weighted magnetic resonance imaging of sacral insufficiency fractures: comparison with metastases of the sacrum. *Spine*. 2007;32(26):E820–824.
22. Castillo M, Arbelaez A, Smith JK, Fisher LL. Diffusion-weighted MR imaging offers no advantage over routine noncontrast MR imaging in the detection of vertebral metastases. *AJNR Am J Neuroradiol*. 2000;21(5):948–53.
23. Baur A, Dietrich O, Reiser M. Diffusion-weighted imaging of the spinal column. *Neuroimaging Clin N Am*. 2002;12(1):147–60.
24. Baur A, Dietrich O, Reiser M. Diffusion-weighted imaging of bone marrow: current status. *Eur Radiol*. 2003;13(7):1699–708.
25. Chan JHM, Peh WCG, Tsui EYK, Chau LF, Cheung KK, Chan KB, et al. Acute vertebral body compression fractures: discrimination between benign and malignant causes using apparent diffusion coefficients. *Br J Radiol*. 2002;75(891):207–14.
26. Pui MH, Mitha A, Rae WID, Corr P. Diffusion-weighted magnetic resonance imaging of spinal infection and malignancy. *J Neuroimaging*. 2005;15(2):164–70.
27. Baur A, Huber A, Dürr HR, Nikolaou K, Stäbler A, Deimling M, et al. Differentiation of benign osteoporotic and neoplastic vertebral compression fractures with a diffusion-weighted, steady-state free precession sequence. *Rofo*. 2002;174(1):70–5.
28. Bhugalo A, Abdullah B, Siow Y, Kh N. Diffusion weighted MR imaging in acute vertebral compression fractures: differentiation between malignant and benign causes. *Biomed Imaging Interv J*. 2006;2(2):e12.
29. Park S, Lee J, Ehara S, Park Y, Sung SO, Choi J, et al. Single shot fast spin echo diffusion-weighted MR imaging of the spine: is it useful in differentiating malignant metastatic tumor infiltration from benign fracture edema? *Clin Imaging*. 2004;28(2):102–8.
30. Jung H, Jee W, McCauley TR, Ha K, Choi K. Discrimination of metastatic from acute osteoporotic compression spinal fractures with MR imaging. *Radiographics*. 2003;23(1):179–87.
31. An HS, Andreshak TG, Nguyen C, Williams A, Daniels D. Can we distinguish between benign versus malignant compression fractures of the spine by magnetic resonance imaging? *Spine*. 1995;20(16):1776–82.
32. Shih TT, Huang KM, Li YW. Solitary vertebral collapse: distinction between benign and malignant causes using MR patterns. *J Magn Reson Imaging*. 1999;9(5):635–42.
33. Frager D, Elkin C, Swerdlow M, Bloch S. Subacute osteoporotic compression fracture: misleading magnetic resonance appearance. *Skeletal Radiol*. 1988;17(2):123–6.
34. Cuénod CA, Laredo JD, Chevret S, Hamze B, Naouri JF, Chapaux X, et al. Acute vertebral collapse due to osteoporosis or malignancy: appearance on unenhanced and gadolinium-enhanced MR images. *Radiology*. 1996;199(2):541–9.
35. Herneth AM, Friedrich K, Weidekamm C, Schibany N, Krestan C, Czerny C, et al. Diffusion weighted imaging of bone marrow pathologies. *Eur J Radiol*. 2005;55(1):74–83.
36. Stäbler A, Baur A, Krüger A, Weiss M, Helmberger T, Reiser M. Differential diagnosis of erosive osteochondrosis and bacterial spondylitis: magnetic resonance tomography (MRT). *Rofo*. 1998;168(5):421–8.
37. Yasumoto M, Nonomura Y, Yoshimura R, Haraguchi K, Ito S, Ohashi I, et al. MR detection of iliac bone marrow involvement by malignant lymphoma with various MR sequences including diffusion-weighted echo-planar imaging. *Skeletal Radiol*. 2002;31(5):263–9.
38. Lin C, Itti E, Luciani A, Haioun C, Meignan M, Rahmouni A. Whole-body diffusion-weighted imaging in lymphoma. *Cancer Imaging*. 2010;10:S172–178.
39. Ballon D, Dyke J, Schwartz LH, Lis E, Schneider E, Lauto A, et al. Bone marrow segmentation in leukemia using diffusion and T (2) weighted echo planar magnetic resonance imaging. *NMR Biomed*. 2000;13(6):321–8.
40. van Rijswijk CSP, Kunz P, Hogendoorn PCW, Taminiu AHM, Doornbos J, Bloem JL. Diffusion-weighted MRI in the characterization of soft-tissue tumors. *J Magn Reson Imaging*. 2002;15(3):302–7.
41. Einarsdóttir H, Karlsson M, Wejde J, Bauer H. Diffusion-weighted MRI of soft tissue tumours. *Eur Radiol*. 2004;14(6):959–63.
42. Nagata S, Nishimura H, Uchida M, Sakoda J, Tonan T, Hiraoka K, et al. Diffusion-weighted imaging of soft tissue tumors: usefulness of the apparent diffusion coefficient for differential diagnosis. *Radiat Med*. 2008;26(5):287–95.
43. Maeda M, Matsumine A, Kato H, Kusuzaki K, Maier SE, Uchida A, et al. Soft-tissue tumors evaluated by line-scan diffusion-weighted imaging: influence of myxoid matrix on the apparent diffusion coefficient. *J Magn Reson Imaging*. 2007;25(6):1199–204.
44. Oka K, Yakushiji T, Sato H, Yorimitsu S, Hayashida Y, Yamashita Y, et al. Ability of diffusion-weighted imaging for the differential diagnosis between chronic expanding hematomas and malignant soft tissue tumors. *J Magn Reson Imaging*. 2008;28(5):1195–200.
45. Dudeck O, Zeile M, Pink D, Pech M, Tunn P, Reichardt P, et al. Diffusion-weighted magnetic resonance imaging allows monitoring of anticancer treatment effects in patients with soft-tissue sarcomas. *J Magn Reson Imaging*. 2008;27(5):1109–13.
46. Baur A, Huber A, Arbogast S, Dürr HR, Zysk S, Wendtner C, et al. Diffusion-weighted imaging of tumor recurrences and post-

- therapeutical soft-tissue changes in humans. *Eur Radiol.* 2001;11(5):828–33.
47. Murphey MD, Flemming DJ, Boyea SR, Bojescul JA, Sweet DE, Temple HT. Enchondroma versus chondrosarcoma in the appendicular skeleton: differentiating features. *Radiographics.* 1998;18(5):1213–37.
 48. Hayashida Y, Hirai T, Yakushiji T, Katahira K, Shimomura O, Imuta M, et al. Evaluation of diffusion-weighted imaging for the differential diagnosis of poorly contrast-enhanced and T2-prolonged bone masses: initial experience. *J Magn Reson Imaging.* 2006;23(3):377–82.
 49. Franzius C, Sciuk J, Daldrup-Link HE, Jürgens H, Schober O. FDG-PET for detection of osseous metastases from malignant primary bone tumours: comparison with bone scintigraphy. *Eur J Nucl Med.* 2000;27(9):1305–11.
 50. Daldrup-Link HE, Franzius C, Link TM, Laukamp D, Sciuk J, Jürgens H, et al. Whole-body MR imaging for detection of bone metastases in children and young adults: comparison with skeletal scintigraphy and FDG PET. *AJR Am J Roentgenol.* 2001;177(1):229–36.
 51. Picci P, Bacci G, Campanacci M, Gasparini M, Pilotti S, Cerasoli S, et al. Histologic evaluation of necrosis in osteosarcoma induced by chemotherapy. Regional mapping of viable and nonviable tumor. *Cancer.* 1985;56(7):1515–21.
 52. Uhl M, Saueressig U, Koehler G, Kontny U, Niemeyer C, Reichardt W, et al. Evaluation of tumour necrosis during chemotherapy with diffusion-weighted MR imaging: preliminary results in osteosarcomas. *Pediatr Radiol.* 2006;36(12):1306–11.
 53. Uhl M, Saueressig U, van Buijen M, Kontny U, Niemeyer C, Köhler G, et al. Osteosarcoma: preliminary results of in vivo assessment of tumor necrosis after chemotherapy with diffusion- and perfusion-weighted magnetic resonance imaging. *Invest Radiol.* 2006;41(8):618–23.
 54. Hayashida Y, Yakushiji T, Awai K, Katahira K, Nakayama Y, Shimomura O, et al. Monitoring therapeutic responses of primary bone tumors by diffusion-weighted image: initial results. *Eur Radiol.* 2006;16(12):2637–43.
 55. Oka K, Yakushiji T, Sato H, Hirai T, Yamashita Y, Mizuta H. The value of diffusion-weighted imaging for monitoring the chemotherapeutic response of osteosarcoma: a comparison between average apparent diffusion coefficient and minimum apparent diffusion coefficient. *Skeletal Radiol.* 2010;39(2):141–6.
 56. Fletcher BD, Wall JE, Hanna SL. Effect of hematopoietic growth factors on MR images of bone marrow in children undergoing chemotherapy. *Radiology.* 1993;189(3):745–51.
 57. Ballon D, Watts R, Dyke JP, Lis E, Morris MJ, Scher HI, et al. Imaging therapeutic response in human bone marrow using rapid whole-body MRI. *Magn Reson Med.* 2004;52(6):1234–8.
 58. Oner AY, Tali T, Celikyay F, Celik A, Le Roux P. Diffusion-weighted imaging of the spine with a non-carr-purcell-meiboom-gill single-shot fast spin-echo sequence: initial experience. *AJNR Am J Neuroradiol.* 2007;28(3):575–80.
 59. Tang G, Liu Y, Li W, Yao J, Li B, Li P. Optimization of b value in diffusion-weighted MRI for the differential diagnosis of benign and malignant vertebral fractures. *Skeletal Radiol.* 2007;36(11):1035–41.
 60. Zhou XJ, Leeds NE, McKinnon GC, Kumar AJ. Characterization of benign and metastatic vertebral compression fractures with quantitative diffusion MR imaging. *AJNR Am J Neuroradiol.* 2002;23(1):165–70.
 61. Raya JG, Dietrich O, Birkenmaier C, Sommer J, Reiser MF, Baur-Melnyk A. Feasibility of a RARE-based sequence for quantitative diffusion-weighted MRI of the spine. *Eur Radiol.* 2007;17(11):2872–9.
 62. Herneth AM, Naude J, Philipp M, Beichel R, Trattng S, Imhof H. The value of diffusion-weighted MRT in assessing the bone marrow changes in vertebral metastases. *Radiologe.* 2000;40(8):731–6.
 63. Herneth AM, Philipp MO, Naude J, Funovics M, Beichel RR, Bammer R, et al. Vertebral metastases: assessment with apparent diffusion coefficient. *Radiology.* 2002;225(3):889–94.
 64. Balliu E, Vilanova JC, Peláez I, Puig J, Remollo S, Barceló C, et al. Diagnostic value of apparent diffusion coefficients to differentiate benign from malignant vertebral bone marrow lesions. *Eur J Radiol.* 2009;69(3):560–6.